www.sciencemag.org/cgi/content/full/336/6088/1573/DC1

# Supplementary Material for

## Baseline Map of Carbon Emissions from Deforestation in Tropical Regions

Nancy L. Harris,* Sandra Brown, Stephen C. Hagen, Sassan S. Saatchi, Silvia Petrova, William Salas, Matthew C. Hansen, Peter V. Potapov, Alexander Lotsch

*To whom correspondence should be sent. E-mail: nharris@winrock.org

Published 22 June 2012, *Science* **336**, 1573 (2012)
DOI: 10.1126/science.1217962

**This PDF file includes:**

## Materials and Methods

### *Geographic extent, definitions, and carbon pools*

Our study region is defined by country and not by biome (Fig. S1). Therefore, the humid and dry tropics as well as small areas of the temperate biome are included.

We use a consistent forest definition across the study region. Forest cover is defined as 25% or greater canopy closure at the Landsat pixel scale (30 m x 30 m spatial resolution) for trees >5 m in height. All tree cover assemblages that met a 25% c anopy closure definition, whether intact forests, plantations, or forest regrowth, are defined as forest *(13-14)*. Deforestation is defined as the reduction to below this 25% threshold *(13-14)*.

Our analysis includes the aboveground biomass of trees with diameter at breast height (DBH) > 10 cm *(15)* as well as belowground tree biomass, as estimated from aboveground values *(17)*. Litter and dead wood pools were excluded due to insufficient data availability. Soil emissions (described below) were excluded due to the generally unquantifiable uncertainty associated with available soil datasets that cover the extent of our study region as well as uncertainty associated with identifying the fate of converted lands after deforestation.

### *Gross vs. Net Estimates*

Estimates of carbon emissions from deforestation require information on both the quantity of forest loss over time and the changes in carbon stocks on land that is cleared. Both terms (area and changes in carbon stocks) can be represented on a gross or net basis.

Inventory statistics such as FAO Forest Resource Assessments (FAO FRA) report net changes in forest area based on the FAO definition of forests (tree crown cover greater than 10%, area more than 0.5 hectares and minimum height of 5 meters at maturity), which account for simultaneous losses and gains in forest area over a given time interval. For example, according to FAO FRA statistics, net forest area in India increased from 64 to 68 million hectares from 1990 to 2005 while net forest area in Brazil decreased from 520 to 478 million hectares during the same time interval. This is not to say that India had no losses in forest cover or that Brazil had no gains in forest cover, but rather forest gains exceeded forest losses in India while forest losses exceeded forest gains in Brazil. In contrast, gross loss in forest area considers only the areas that were classified as forest at the beginning of a defined time interval and then converted to non-forest by the end of the time interval. In other words, estimates of gross forest cover loss do not consider concomitant gains in forest area elsewhere. Remote sensing based approaches to tracking changes in forest area over time can disaggregate forest losses from forest gains more easily than standard inventory approaches. Policy mechanisms for reducing carbon emissions in developing countries call for forest area change estimates that are broken down into separate forest loss and forest gain categories rather than a simple value of the net change in forest area. To ensure that our analysis is relevant to international policy, we focus our analysis on gross forest loss.

Two options also exist for estimating resulting carbon emissions from gross forest loss: (1) net emissions, in which losses, storage and gains of carbon are considered as a result of a change in land use; and (2) gross emissions, which include only losses of carbon without consideration of carbon storage (such as occurs in long-term wood products) or consideration of carbon gains (such as occurs in re-growing vegetation). We focus our analysis on gross emissions because we can generate clear, statistically-based uncertainty bounds around these estimates with the data and methods that are currently available. Net emissions estimates require assumptions about the fate of converted lands to determine net carbon impacts, which currently cannot be ascertained with statistical confidence across large regions. The effect of incorporating assumptions about the fate of converted lands to generate a net emissions estimate would be a reduction in our estimate of gross carbon emissions from deforestation.

Table S1 summarizes existing estimates of carbon emissions from tropical deforestation and provides some insight into why our estimates differ from other published ones. All published estimates of net and gross emissions from tropical deforestation, including those most recently published in (*11-12*), rely on the same bookkeeping model that tracks carbon dynamics following tropical land-use change using coefficients defined by region (South and Central America, Tropical Africa, and South and Southeast Asia) and by broad ecosystem type (tropical evergreen, seasonal and open forest in South and Central America; closed and open forest in Tropical Africa, and tropical moist, seasonal and open forest in South and Southeast Asia). Most recently, the authors of (*12*) use the same forest loss product as we use in this analysis (*13-14*), but only as a means for spatially locating forests on their aboveground carbon stock map [derived independently of the map used in our analysis (*15*)] that had been recently deforested. The authors of *(12)* proposed that this step produced more representative biomass values for their modeled regions, as they better identified the areas that already have been deforested or are at high risk for deforestation. The revised regional biomass values were then combined in the bookkeeping model with FAO data that report net (not gross) loss in forest area and are based on a different definition of forest than used in (*13-14*). In contrast, our analysis co-locates remote sensing based biomass density and forest loss information at high spatial resolution (18.5 km) and overcomes the resolution mismatch in the data by applying a randomization procedure (refer to next section below for additional details). Rather than making assumptions about the fate of the cleared carbon and tracking carbon dynamics through time, we simplify the calculation of (gross) carbon emissions as the area of gross forest loss multiplied by the carbon stock of the forest prior to clearing.

***Approach for estimating gross carbon emissions***

We estimate deforestation using a map of gross forest cover loss (GFCL) *(13-14)*. The methodology used to generate the map is based on a stratified random sample of 18.5 x 18.5-km blocks and employs data from two satellite-based sensors. Coarse spatial resolution data from the MODIS (Moderate Resolution Imaging Spectroradiometer) sensor enable stratification of the earth's forested biomes into multiple sub-regions, or strata, ranging from low to high probability of forest cover loss. Stratum breakpoints were selected independently for each biome. Within each stratum, Landsat Enhanced Thematic Mapper Plus (ETM+) data were obtained for the sampled blocks within each stratum and provided the primary data for quantifying GFCL between 2000 and 2005. The standard errors of GFCL estimates are generally sufficiently low to

indicate that the combination of MODIS-based stratification with poststratified and regression estimators resulted in precise estimates of area of GFCL *(14)*. Additional details on the GFCL product are available in *(14)*.

Above and belowground forest biomass carbon stocks across the study region are estimated using a 1-km resolution map derived for the early 2000s created from ground inventory data, lidar observations, and optical and microwave satellite imagery *(15)*. The 1-km resolution carbon stock maps were directly associated with the forest loss map at the 18.5-km block scale using a randomization technique (see discussion of Uncertainty from other sources below).

We estimate carbon emissions from deforestation for the period 2000 to 2005 as the product of GFCL and forest biomass carbon stocks. We resolve the disparate spatial resolution of these two maps by repeating a randomization procedure (n=1,000), in which forested 1-km pixels within a given 18.5-km block are selected randomly until the forest loss quota for the block (in ha) is met. The carbon values of the selected 1-km pixels (in Mg C) are then summed across the block to derive an emissions estimate. The average of the 1,000 estimates of carbon emissions associated with forest loss is assigned as the best estimate per 18.5-km block. We assume that all carbon in above and belowground biomass is emitted immediately to the atmosphere at the time of clearing *(21)*; we do not attempt to track the fate of all carbon pools through time.

***Approach for estimating uncertainty***

We generate uncertainty bounds around our final emissions estimate using a randomized, Monte Carlo style sampling technique *(25-26)*. In each scenario of the simulation, forested pixels (1-km) within each 18.5-km block are selected randomly until the total cleared area estimated within the block is reached. Carbon stock information for the cleared pixels is then used to calculate an emissions estimate associated with forest loss for that scenario. Iterating through scenarios for each block results in a distribution of emissions associated with the estimated level of forest loss (Fig. S2). This approach allows us to combine uncertainty from different sources without making assumptions about the distribution of the underlying data. We incorporate uncertainty from the following components:

1. Estimates of forest loss *(13-14)*;
2. Estimates of aboveground biomass *(15)*;
3. Estimates of belowground biomass *(17)*

We use a series of distributions representing uncertainty from each of these three main sources to construct 1,000 scenarios. At the conclusion of our simulation, each of the 1,000 scenarios exists as a full resolution (18.5-km) map of carbon lost to the atmosphere as a result of forest loss between 2000 and 2005. From these 1,000 scenario maps, we construct the 90% prediction limits at the block, country, regional, and pan-continental scales by first aggregating each individual map to the targeted scale (e.g., country, continent) and then selecting the 0.05 and 0.95 percentiles (i.e., $50^{th}$ and $950^{th}$ out of 1,000 sorted simulations). The identification of the 0.05 and 0.95 percentile values is computed individually for GFCL, carbon stock, and emissions, such that the low emission value is not simply a combination of the low bound for GFCL and the low bound for carbon stocks; it is the $50^{th}$ out of 1,000 sorted simulations that combined GFCL and

carbon stock. The distributions from which randomized selections are drawn during this simulation are estimated during the model fitting and validation processes. The distributions from each of the three sources are constructed in different ways (described below).

Uncertainty in forest loss

Uncertainty in the forest loss product is estimated from the modeled relationship between two estimates of forest loss at the 18.5-km block scale, one derived from coarse resolution Moderate Resolution Imaging Spectroradiometer (MODIS) imagery and the other from higher resolution Landsat imagery. Full details regarding this modeling process are available in *(13-14)*. In summary, each biome was divided into forest cover loss strata based on MODIS observations, and included high, medium and low forest cover loss strata per biome. A stratified random sample of 18.5-km blocks was then selected from each biome and stratum, and Landsat imagery was analyzed to quantify forest cover loss per sample block. Stratum-specific regression estimators incorporating MODIS-indicated forest cover loss as the auxiliary variables were applied to generate forest cover loss estimates over the global population of 18.5-km blocks. To conduct the uncertainty analysis, we use a bootstrapping approach (i.e. resampling with replacement) (*25*,*27*), which assumes that the observed data represent only one possible realization out of many, and reconstructs a large number of alternate realizations based on random resampling of residuals. Here, we use bootstrapping on the original forest loss data and model to create a distribution of regression parameters for each forest cover loss stratum. When creating each of the 1,000 scenarios, we draw a single estimate of possible regression parameters to use within the stratum for that scenario. To extend this estimate to prediction intervals that take into account additional uncertainty due to inherent variations in the data, we add a randomly drawn residual from the model residuals to each predicted pixel's forest loss value in each scenario (Fig. S2A). It is important to note that this uncertainty analysis does not explicitly include uncertainty in the Landsat maps of forest loss, i.e., Landsat maps are taken as 'true'.

Uncertainty in aboveground biomass

The aboveground biomass map used for this study *(15)* is at 1-km spatial resolution (100 ha pixels) and provides the best available estimate of biomass (in Mg C $ha^{-1}$) and associated uncertainties at the same spatial resolution across the tropics. Uncertainties are derived from a bootstrapping exercise conducted as part of the Maximum Entropy (MaxEnt) model estimator through an error propagation approach and from an independent model validation analysis. Full details of the MaxEnt approach are available in *(15)*. For each pixel we calculate a minimum and maximum possible biomass value that includes a potential bias in the initial data used to train the model (see below). The values represent the 0.5 percentile (minimum) and the 99.5 percentile (maximum) of an assumed Gaussian distribution of errors at the pixel scale (Fig. S2B). This range of potential error accounts for uncertainty from several sources, including the estimates of vegetation height from the Geoscience Laser Altimeter System (GLAS), onboard the Ice, Cloud, and land Elevation Satellite (ICESat), lidar data, allometric equations used to convert height to aboveground biomass, and prediction errors associated with the MaxEnt model estimator. The potential bias in the model estimate of forest biomass can be related to the ground estimates of biomass used in calibrating the GLAS lidar data or the inventory plots used directly in the MaxEnt model. This bias cannot be quantified systematically due to lack of detailed information

on inventory data and the paucity of ground measurements of forest biomass to evaluate the estimates. However, by using the estimate of the potential bias and introducing it in computing emissions, we ensure the overall estimates of regional and national emissions are reliable. For our analysis, we estimate continent-wide potential bias by averaging the pixel values of minimum and maximum biomass over the continent and differencing these averages from the original (i.e., median or "best estimate") biomass map. These minimum and maximum pixel level bias values are used to represent the distribution of potential bias over each continent. When creating each of the 1,000 scenarios, we draw a single estimate of bias from the Gaussian distribution of potential biases to apply to all pixels within the continent for that scenario. This provides an estimate of the confidence limits around a mean response. To extend this estimate to prediction intervals that take into account additional uncertainty due to inherent variations in the data, we add a randomly drawn residual from the MaxEnt model to each predicted pixel biomass value in each scenario.

We also performed an independent validation of the MaxEnt estimated biomass map (100 ha pixels) by examining more than 65,000 additional estimates of biomass derived from the GLAS lidar points (<0.25 ha footprints) distributed across the three regions. These lidar-derived estimates of biomass were not used in the MaxEnt model training *(15)*. Our analysis showed that the MaxEnt estimated biomass map was biased downward by 7.9, 16.1, and 11.7 Mg C $ha^{-1}$ in the Americas, Africa, and Asia, respectively. We corrected all 1,000 scenarios for this identified bias. The bias is based on three potential sources: (1) the spatial footprint of the lidar point measurements (<0.25 ha) is different from the spatial scale of the biomass map based on the coarse resolution remote sensing imagery (100 ha); (2) due to heterogeneity of forest cover within the 100 ha pixels, the average biomass density of the pixel is often lower than the biomass density of smaller areas of forest measured within the pixel; (3) the remote sensing data used to estimate or extrapolate the ground and lidar measurements over the landscape often have less sensitivity to high forest biomass density and tend to underestimate the biomass over the landscape. Theoretically, the bias can be reduced or taken into account in quantifying the local and regional carbon stocks using bias reduction algorithms *(28)*. However, we expect the use of higher resolution imagery (~100 m) to extrapolate the lidar derived biomass point or ground estimates of biomass over the landscape can potentially significantly reduce the bias in modeling forest biomass with remote sensing data. In summary, the bias is not due to the MaxEnt modeling process, but to the difference between the scale of the map (100 ha) and the scale of GLAS biomass values derived from <0.25 ha footprints. We included this bias in our emissions estimation scenarios to compensate for the potential underestimation of emissions that could result by excluding deforestation events occurring at scales smaller than the 100 ha pixels for which forest biomass carbon stocks were estimated. If deforestation occurred at the same scale as the biomass map was generated (100 ha), the need for compensating for this bias may not have been necessary.

Uncertainty in belowground biomass

Belowground tree biomass is estimated from aboveground biomass using a regression equation developed from field data collected in forests across multiple biomes *(17)*. Uncertainties in this relationship between above and belowground biomass are estimated from the original model fit *(17)*; the model fits a power function to above and belowground biomass data using least squares

regression. Here, we follow the same bootstrapping approach implemented for forest loss uncertainty to create a distribution of regression coefficients *(25,27)*. When creating each of the 1,000 scenarios, we draw a single estimate of regression coefficients relating above- to belowground biomass to apply to all pixels within that scenario. To extend this estimate to prediction intervals that take into account additional uncertainty due to inherent variations in the data, we add a randomly drawn residual from the model residuals to each predicted pixel's belowground biomass value in each scenario (Fig. S2B).

Uncertainty from other sources

Our simulation accounts for an additional source of uncertainty related to spatial scale. Because our forest loss estimates are at the 18.5-km scale and our biomass estimates are at the 1-km scale, there is uncertainty in which specific 1-km forest areas were deforested within the 18.5-km block. We estimate the uncertainty from this lack of spatial specificity using randomization. For each 18.5-km block within each of the 1,000 scenarios, we randomly select a group of 1-km areas within the block for deforestation until the forest loss quota is met. We screen the 1-km biomass data with the MODIS 2000 Vegetation Continuous Fields Tree Cover data *(29)* using a filter of 25%, meaning that all 1-km pixels within the 18.5-km block have a uniform chance of being selected for deforestation if they have an estimated tree cover percentage of 25% or higher.

### *Emissions and Removals from Converted Lands*

Carbon emissions from soil occur when forest land on mineral soil is converted to annual cropland and/or when organic soils are drained and burned for agricultural production *(21)*. Although we exclude soil carbon emissions from our estimate of carbon emissions from deforestation, we provide a first-order estimate of carbon emissions from mineral soils by assuming all areas of forest loss between 2000 and 2005 are converted to annual cropland.

We use a standard methodology for estimating emissions from mineral soils *(21)* and a global database on soil carbon stocks *(19)* to evaluate the extent to which carbon emissions from mineral soils could influence our total emissions estimate. Because the specific year of forest loss over the time period 2000 to 2005 over the study region was unknown, we assume an average of 2.5 years of soil carbon emissions (i.e., the midpoint of the time period analyzed) and used the median initial soil carbon stock of 50 t C $ha^{-1}$ for the study region. Assuming that all forest lost between 2000 and 2005 across the study region was converted to annual cropland, carbon emissions from mineral soils between 2000 and 2005 would add an additional 4% (0.03 Pg C $yr^{-1}$) to our deforestation emissions estimate.

Emissions from the drainage and burning of peat soils in southeast Asia has contributed substantially to global greenhouse gas emissions in past decades *(22)*. Because the forest loss estimates used in our emissions analysis are produced at the 18.5-km block scale, it is not possible to identify which specific forested pixels were cleared for cropland within a block, let alone identify which pixels were cleared for cropland *on peat* within a block. Therefore, we use peer-reviewed estimates of emissions from peat fire *(23)* and peat drainage *(24)* that were

generated for an overlapping time period to our analysis (2000-2006) to estimate peat emissions as 0.3 Pg C $yr^{-1}$.

Removals of carbon from the atmosphere occur when vegetation is established on land after a deforestation event has occurred. This vegetation could include annual or perennial crops, grasses or woody plants. We exclude these removals from our estimates of gross carbon emissions, but provide a first-order approximation of their magnitude by assuming, as with soil, that all lands are converted to annual croplands. We use a standard methodology and default value of 5 t C $ha^{-1}$ *(21)* to assign post-deforestation carbon stocks across the study region. Accounting for these removals would reduce our gross emissions estimate by 5% (0.04 Pg C $yr^{-1}$). Changing the assumption to a land cover type with higher carbon stocks (such as forest regrowth) would further reduce our estimate of gross carbon emissions.

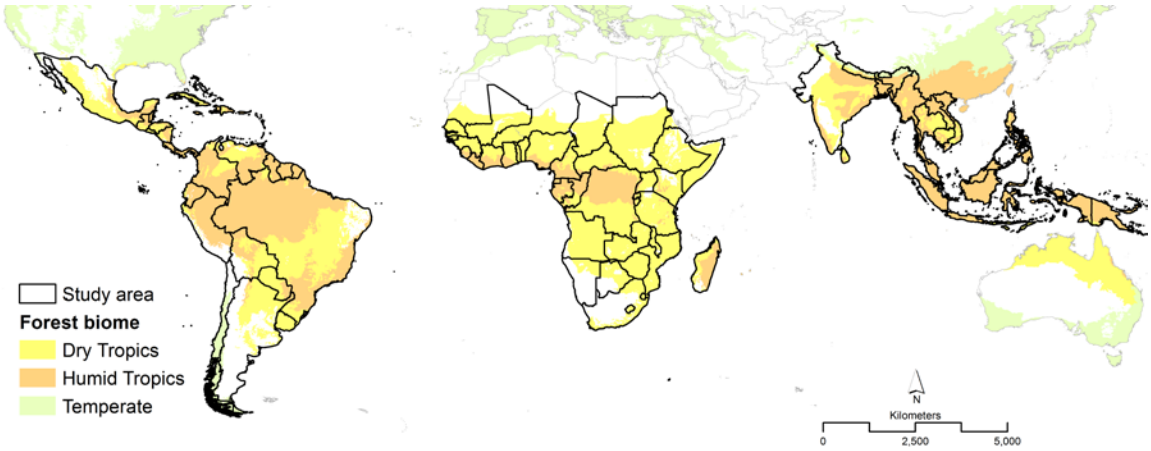


**Fig. S1.**

Countries included in the analysis of carbon emissions from deforestation. The humid tropics, dry tropics and temperate forest biomes account for 61, 37 and 2% of the study area, respectively.

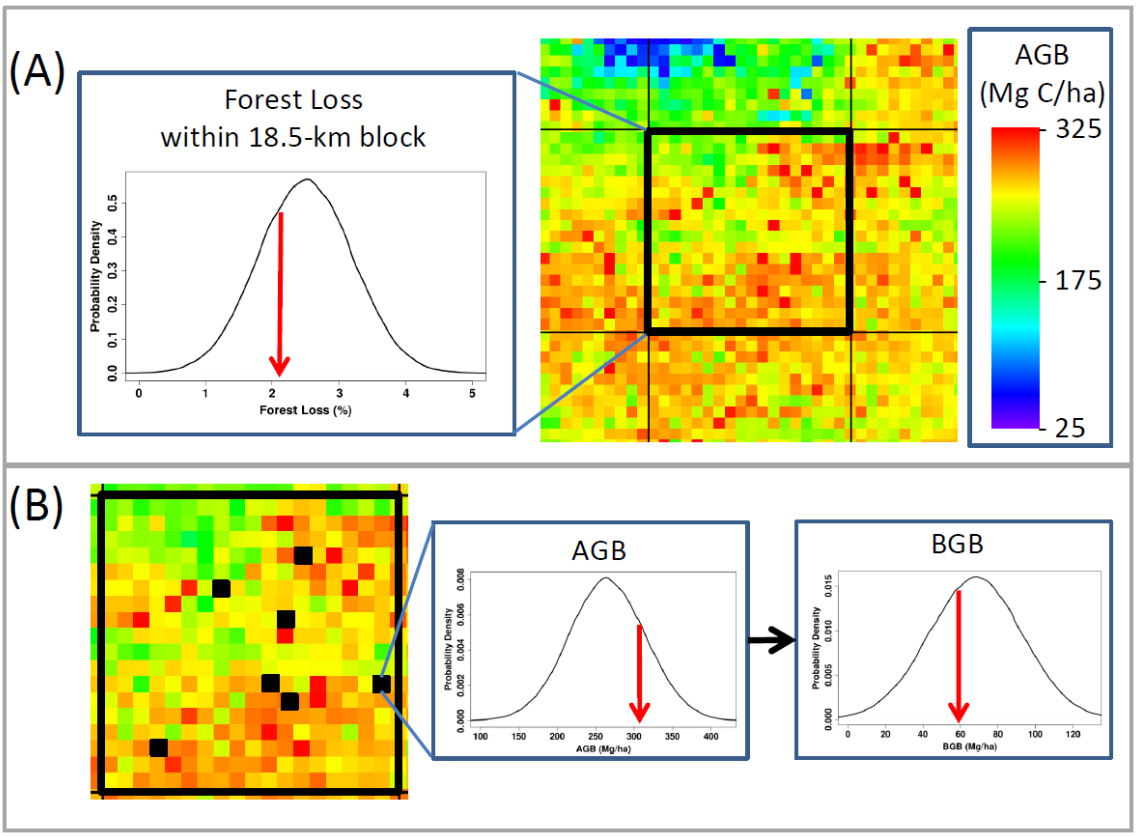


**Fig. S2.** Illustration of one scenario of the Monte Carlo style uncertainty analysis developed to estimate carbon emissions from deforestation. (A) Estimates of forest loss are available at the 18.5-km block scale (black grid) while carbon stock estimates are available at the 1-km scale (colored pixels). The forest loss estimate for each block exists as a distribution rather than as a single value; the red arrow illustrates one random draw (out of 1,000) for the forest loss estimate per block. (B) After a single value of forest loss per block is selected randomly from the distribution in (A), 1-km forested pixels within the block are selected randomly for biomass removal (black pixels) until the forest loss quota defined in (A) is met. A random draw from the distribution of aboveground biomass (AGB) values for each selected 1-km pixel (AGB; red arrow) is used as the aboveground biomass estimate for the scenario. A belowground biomass (BGB) value (BGB; red arrow) is then selected from the distribution of BGB values generated using a relationship derived between ABG and BGB *(17)*.

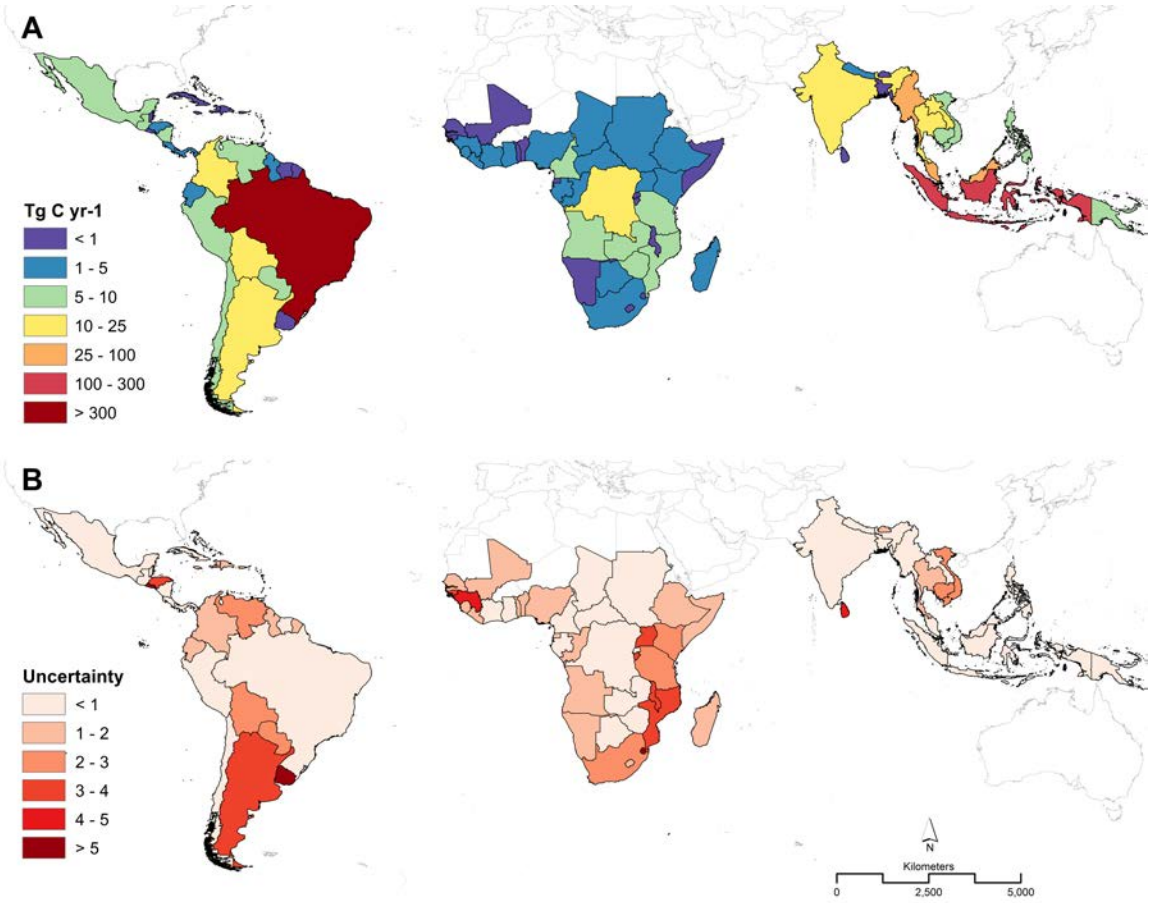


**Fig. S3.** Relative ordering of (A) deforestation emissions between 2000 and 2005 and (B) uncertainty in emissions estimates by country. Uncertainty is estimated as the ratio of the range of emission values within the 90% prediction interval to the median emissions estimate.

**Table S1.**

Comparison of estimates from carbon emissions from land-cover change.

| Study | Forest Area Change (Net/Gross) | Carbon Emissions (Net/Gross) | Emissions Estimate (Pg C $yr^{-1}$) | Time Period |
|---|---|---|---|---|
| Houghton et al. (2003)* | Net | Net | 2.2 ± 0.6 | 1990s |
| DeFries et al. (2002)* | Gross | Net | 0.9 ± 0.5 | 1990s |
| Achard et al. (2004)* | Gross | Net | 1.1 ± 0.3 | 1990s |
| Van der Werf et al. (2009) | Gross | Net | 1.2 | 2000-2005 |
| Friedlingstein et al. (2010)* | Net | Net | 1.1 ± 0.7 | 2000-2009 |
| Pan et al. (2011)* | Net | Net + Gross | 1.3 ± 0.7 (Net)<br>2.8 ± 0.5 (Gross) | 2000-2007 |
| Baccini et al. (2012) | Net | Net + Gross | 1.0 (Net)<br>2.2 (Gross) | 2000-2010 |
| This study† | Gross | Gross | 0.81 (median)<br>0.57 – 1.22 (range) | 2000–2005 |

***** Uncertainty based on expert opinion

† Uncertainty based on statistical analysis

**Table S2.**

Country level estimates of forest area in the year 2000 *(14)*, gross forest cover loss from 2000-2005 *(14)*, above- and belowground biomass carbon stocks in the year 2000 *(15)*, and emissions from deforestation from 2000-2005. Low and high estimates represent the 90% prediction interval, which are derived from a Monte Carlo style sampling technique that includes all critical sources of uncertainty. Low, mean and high forest carbon stock values are generated for forests with at least 25% tree cover by integrating potential systematic errors associated with pixel (1-km)-level biomass carbon estimates.

| Country | Forest Area 2000 (Mha) | Gross Forest Cover Loss (000 ha $yr^{-1}$) | | | Forest Carbon Stock Density (Mg C $ha^{-1}$) | | | Emissions from Deforestation (Tg C $yr^{-1}$) | | |
|---|---|---|---|---|---|---|---|---|---|---|
| | | Low | Median | High | Low | Mean | High | Low | Median | High |
| Angola | 49 | 56 | 126 | 199 | 46 | 47 | 49 | 3 | 6 | 12 |
| Benin | 2 | 6 | 12 | 18 | 29 | 29 | 29 | 0 | 0 | 1 |
| Botswana | 4 | 36 | 48 | 59 | 19 | 19 | 19 | 1 | 1 | 2 |
| Burundi | 1 | 0 | 3 | 7 | 59 | 64 | 71 | 0 | 0 | 1 |
| Cote d'Ivoire | 8 | 25 | 39 | 53 | 78 | 85 | 92 | 2 | 3 | 4 |
| Cameroon | 26 | 35 | 54 | 74 | 131 | 142 | 154 | 4 | 7 | 10 |
| CAR | 36 | 43 | 65 | 88 | 60 | 66 | 73 | 3 | 4 | 7 |
| Chad | 5 | 23 | 37 | 50 | 31 | 31 | 32 | 1 | 1 | 2 |
| Dem. Rep. Congo | 167 | 120 | 203 | 289 | 116 | 128 | 138 | 16 | 23 | 32 |
| Equatorial Guinea | 2 | 1 | 3 | 5 | 148 | 160 | 173 | 0 | 1 | 1 |
| Ethiopia | 16 | 24 | 68 | 115 | 49 | 53 | 58 | 1 | 4 | 7 |
| Gabon | 19 | 12 | 24 | 35 | 152 | 164 | 177 | 2 | 4 | 6 |
| Gambia | 0 | 0 | 1 | 2 | 12 | 12 | 12 | 0 | 0 | 0 |
| Ghana | 5 | 18 | 30 | 43 | 86 | 94 | 103 | 1 | 2 | 3 |
| Guinea | 9 | 0 | 27 | 101 | 53 | 57 | 63 | 0 | 2 | 7 |
| Guinea-Bissau | 1 | 0 | 2 | 7 | 37 | 37 | 38 | 0 | 0 | 0 |
| Kenya | 4 | 3 | 39 | 78 | 50 | 54 | 57 | 0 | 2 | 4 |
| Lesotho | 1 | 1 | 3 | 4 | 19 | 19 | 19 | 0 | 0 | 0 |
| Liberia | 7 | 7 | 14 | 21 | 135 | 147 | 159 | 1 | 2 | 3 |
| Madagascar | 16 | 0 | 52 | 104 | 64 | 70 | 75 | 0 | 3 | 7 |
| Malawi | 2 | 0 | 10 | 28 | 39 | 40 | 42 | 0 | 0 | 2 |
| Mali | 3 | 17 | 28 | 39 | 43 | 44 | 46 | 1 | 1 | 2 |
| Mozambique | 34 | 0 | 196 | 617 | 41 | 42 | 43 | 0 | 9 | 35 |
| Namibia | 1 | 10 | 17 | 24 | 16 | 16 | 16 | 0 | 0 | 1 |
| Nigeria | 12 | 46 | 81 | 118 | 75 | 83 | 91 | 2 | 4 | 7 |
| Rep. of Congo | 23 | 0 | 26 | 62 | 147 | 160 | 171 | 0 | 3 | 6 |
| Rwanda | 0 | 2 | 3 | 4 | 66 | 73 | 81 | 0 | 0 | 0 |
| Senegal | 2 | 8 | 14 | 20 | 26 | 26 | 26 | 0 | 0 | 1 |
| Sierra Leone | 3 | 1 | 16 | 31 | 75 | 83 | 92 | 0 | 1 | 3 |
| Somalia | 1 | 9 | 20 | 32 | 34 | 34 | 34 | 0 | 1 | 2 |
| South Africa | 13 | 0 | 99 | 203 | 27 | 28 | 29 | 0 | 4 | 11 |
| Sudan | 17 | 59 | 95 | 130 | 43 | 45 | 47 | 3 | 4 | 6 |
| Swaziland | 1 | 0 | 2 | 15 | 32 | 32 | 33 | 0 | 0 | 1 |
| Tanzania | 23 | 0 | 149 | 297 | 44 | 45 | 47 | 0 | 7 | 17 |

| Country | Forest Area 2000 (Mha) | Gross Forest Cover Loss (000 ha $yr^{-1}$) | | | Forest Carbon Stock Density (Mg C $ha^{-1}$) | | | Emissions from Deforestation (Tg C $yr^{-1}$) | | |
|---|---|---|---|---|---|---|---|---|---|---|
| | | Low | Median | High | Low | Mean | High | Low | Median | High |
| Togo | 1 | 3 | 6 | 9 | 46 | 49 | 53 | 0 | 0 | 0 |
| Uganda | 5 | 0 | 23 | 67 | 59 | 65 | 71 | 0 | 1 | 5 |
| Zambia | 29 | 93 | 134 | 176 | 43 | 43 | 44 | 5 | 7 | 11 |
| Zimbabwe | 9 | 78 | 119 | 161 | 29 | 30 | 30 | 4 | 5 | 8 |
| **Total Africa** | **558** | **737** | **1,889** | **3,387** | **69** | **93** | **117** | **54** | **116** | **218** |
| Argentina | 49 | 0 | 437 | 1064 | 16 | 24 | 32 | 0 | 10 | 33 |
| Belize | 1 | 6 | 9 | 11 | 93 | 105 | 117 | 1 | 1 | 1 |
| Bolivia | 61 | 0 | 129 | 366 | 79 | 90 | 102 | 0 | 11 | 27 |
| Brazil | 458 | 1,495 | 3,292 | 5,089 | 103 | 116 | 129 | 270 | 340 | 481 |
| Chile | 17 | 49 | 67 | 85 | 45 | 52 | 60 | 5 | 6 | 8 |
| Colombia | 63 | 15 | 137 | 258 | 124 | 138 | 152 | 6 | 14 | 26 |
| Costa Rica | 3 | 7 | 12 | 17 | 94 | 105 | 117 | 1 | 1 | 2 |
| Ecuador | 13 | 12 | 37 | 61 | 136 | 149 | 163 | 2 | 4 | 7 |
| El Salvador | 1 | 0 | 2 | 9 | 40 | 49 | 58 | 0 | 0 | 1 |
| French Guiana | 7 | 1 | 2 | 4 | 148 | 160 | 173 | 0 | 0 | 1 |
| Guatemala | 6 | 39 | 50 | 61 | 80 | 92 | 103 | 4 | 5 | 7 |
| Guyana | 16 | 7 | 13 | 18 | 146 | 161 | 176 | 1 | 1 | 2 |
| Honduras | 6 | 0 | 17 | 48 | 67 | 77 | 87 | 0 | 1 | 4 |
| Mexico | 46 | 97 | 140 | 187 | 39 | 48 | 57 | 6 | 8 | 12 |
| Nicaragua | 5 | 20 | 50 | 79 | 100 | 113 | 125 | 4 | 6 | 9 |
| Panama | 3 | 8 | 12 | 16 | 104 | 115 | 126 | 1 | 1 | 2 |
| Paraguay | 21 | 0 | 242 | 497 | 19 | 27 | 35 | 1 | 9 | 21 |
| Peru | 68 | 36 | 57 | 78 | 143 | 158 | 172 | 5 | 7 | 11 |
| Suriname | 12 | 4 | 6 | 8 | 146 | 161 | 176 | 1 | 1 | 1 |
| Uruguay | 3 | 0 | 19 | 125 | 21 | 28 | 36 | 0 | 1 | 7 |
| Venezuela | 49 | 0 | 115 | 359 | 121 | 134 | 147 | 0 | 9 | 25 |
| Caribbean | 7 | 12 | 28 | 45 | 39 | 46 | 53 | 1 | 2 | 3 |
| **Total Latin America** | **915** | **1,809** | **4,873** | **8,488** | **100** | **112** | **125** | **309** | **440** | **674** |
| Bangladesh | 2 | 5 | 7 | 10 | 87 | 94 | 102 | 1 | 1 | 1 |
| Bhutan | 2 | 2 | 4 | 6 | 141 | 152 | 163 | 0 | 1 | 1 |
| Brunei | 0 | 0 | 1 | 1 | 149 | 165 | 180 | 0 | 0 | 0 |
| Cambodia | 9 | 0 | 58 | 149 | 115 | 127 | 138 | 0 | 8 | 19 |
| India | 42 | 142 | 206 | 275 | 96 | 104 | 112 | 14 | 18 | 27 |
| Indonesia | 107 | 556 | 701 | 848 | 141 | 155 | 170 | 87 | 105 | 137 |
| Laos | 16 | 49 | 85 | 121 | 148 | 164 | 179 | 10 | 15 | 21 |
| Malaysia | 22 | 170 | 233 | 296 | 163 | 179 | 195 | 32 | 41 | 55 |
| Nepal | 5 | 10 | 16 | 23 | 95 | 103 | 111 | 1 | 2 | 3 |
| PNG | 31 | 27 | 50 | 73 | 137 | 152 | 167 | 4 | 7 | 11 |
| Philippines | 10 | 24 | 40 | 57 | 109 | 118 | 127 | 3 | 6 | 9 |
| Myanmar | 33 | 139 | 186 | 231 | 141 | 155 | 168 | 23 | 29 | 39 |
| Sri Lanka | 3 | 0 | 7 | 35 | 85 | 94 | 104 | 0 | 1 | 3 |
| Thailand | 17 | 15 | 134 | 250 | 114 | 126 | 137 | 6 | 16 | 29 |

| Country | Forest Area 2000 (Mha) | Gross Forest Cover Loss (000 ha $yr^{-1}$) | | | Forest Carbon Stock Density (Mg C $ha^{-1}$) | | | Emissions from Deforestation (Tg C $yr^{-1}$) | | |
|---|---|---|---|---|---|---|---|---|---|---|
| | | Low | Median | High | Low | Mean | High | Low | Median | High |
| Vietnam | 14 | 0 | 55 | 133 | 115 | 127 | 139 | 0 | 8 | 20 |
| **Total Asia** | **317** | **1,138** | **1,785** | **2,508** | **141** | **155** | **169** | **208** | **257** | **345** |

**References and Notes**


1. G. P. Peters *et al*., Rapid growth in $CO_2$ emissions after the 2008–2009 global financial crisis. *Nature Clim. Change* **2**, 2 (2012). doi:10.1038/nclimate1332

2. R. A. Houghton, K. T. Lawrence, J. L. Hackler, S. Brown, The spatial distribution of forest biomass in the Brazilian Amazon: A comparison of estimates. *Glob. Change Biol.* **7**, 731 (2001). doi:10.1046/j.1365-2486.2001.00426.x

3. Y. Mahli, The carbon balance of tropical forest regions, 1990–2005. *Curr. Op. Environ. Sustain.* **2**, 237 (2010). doi:10.1016/j.cosust.2010.08.002

4. R. A. Houghton *et al*., Changes in the carbon content of terrestrial biota and soils between 1860 and 1980: A net release of $CO_2$ to the atmosphere. *Ecol. Monogr.* **53**, 235 (1983). doi:10.2307/1942531

5. R. A. Houghton *et al*., Net flux of carbon dioxide from tropical forests in 1980. *Nature* **316**, 617 (1985). doi:10.1038/316617a0

6. R. A. Houghton, The annual net flux of carbon to the atmosphere from changes in land use 1850–1990. *Tellus* **51B**, 298 (1999).

7. R. A. Houghton, Revised estimates of the annual net flux of carbon to the atmosphere from changes in land use and land management 1850-2000. *Tellus* **55B**, 378 (2003).

8. A. Grainger, Difficulties in tracking the long-term global trend in tropical forest area. *Proc. Natl. Acad. Sci. U.S.A.* **105**, 818 (2008). doi:10.1073/pnas.0703015105 Medline

9. R. S. DeFries *et al*., Carbon emissions from tropical deforestation and regrowth based on satellite observations for the 1980s and 1990s. *Proc. Natl. Acad. Sci. U.S.A.* **99**, 14256 (2002). doi:10.1073/pnas.182560099 Medline

10. F. Achard, H. D. Eva, P. Mayaux, H.-J. Stibig, A. Belward, Improved estimates of net carbon emissions from land cover change in the tropics for the 1990s. *Global Biogeochem. Cycles* **18**, GB2008 (2004). doi:10.1029/2003GB002142

11. Y. Pan *et al*., A large and persistent carbon sink in the world's forests. *Science* **333**, 988 (2011). doi:10.1126/science.1201609 Medline

12. A. Baccini *et al*., Estimated carbon dioxide emissions from tropical deforestation improved by carbon-density maps. *Nature Clim. Change* **2**, 182 (2012). doi:10.1038/nclimate1354

13. M. C. Hansen *et al*., Humid tropical forest clearing from 2000 to 2005 quantified by using multitemporal and multiresolution remotely sensed data. *Proc. Natl. Acad. Sci. U.S.A.* **105**, 9439 (2008). doi:10.1073/pnas.0804042105 Medline

14. M. C. Hansen, S. V. Stehman, P. V. Potapov, Quantification of global gross forest cover loss. *Proc. Natl. Acad. Sci. U.S.A.* **107**, 8650 (2010). doi:10.1073/pnas.0912668107 Medline

15. S. S. Saatchi *et al*., Benchmark map of forest carbon stocks in tropical regions across three continents. *Proc. Natl. Acad. Sci. U.S.A.* **108**, 9899 (2011). doi:10.1073/pnas.1019576108 Medline

16. Materials and methods are available as supplementary materials on *Science* Online.

17. K. Mokany, R. J. Raison, A. S. Prokushkin, Critical analysis of root:shoot ratios in terrestrial biomes. *Glob. Change Biol.* **12**, 84 (2006). doi:10.1111/j.1365-2486.2005.001043.x

18. M. A. Cairns, S. Brown, E. H. Helmer, G. A. Baumgardner, Root biomass allocation in the world's upland forests. *Oecologia* **111**, 1 (1997). doi:10.1007/s004420050201

19. FAO/IIASA/ISRIC/ISSCAS/JRC. Harmonized World Soil Database (version 1.1); FAO, Rome, Italy and IIASA, Laxenburg, Austria (2009)

20. O. Arino *et al*., GlobCover: ESA service for global land cover from MERIS. Geoscience and Remote Sensing Symposium (IEEE International, IGARSS 2007, 2007).

21. IPCC, IPCC guidelines for national greenhouse gas inventories (IGES, Japan, 2006; www.ipcc-nggip.iges.or.jp/public/2006gl/index.html).

22. S. E. Page *et al*., The amount of carbon released from peat and forest fires in Indonesia during 1997. *Nature* **420**, 61 (2002). doi:10.1038/nature01131 Medline

23. G. R. van der Werf *et al*., Climate regulation of fire emissions and deforestation in equatorial Asia. *Proc. Natl. Acad. Sci. U.S.A.* **105**, 20350 (2008). doi:10.1073/pnas.0803375105 Medline

24. A. Hooijer *et al*., Current and future $CO_2$ emissions from drained peatlands in Southeast Asia. *Biogeosciences* **7**, 1505 (2010). doi:10.5194/bg-7-1505-2010

25. S. C. Hagen *et al*., Statistical uncertainty of eddy-flux based estimates of gross ecosystem carbon exchange at Howland Forest, Maine. *J. Geophys. Res.* **111**, (D8), D08S03 (2006). doi:10.1029/2005JD006154

26. C. P. Robert, G. Casella, *Monte Carlo Statistical Methods* (Springer-Verlag, New York, 1999).

27. B. Efron, R. Tibshirani, Bootstrap methods for standard errors, confidence intervals, and other measures of statistical accuracy. *Stat. Sci.* **1**, 54 (1986). doi:10.1214/ss/1177013815

28. I. Kosmidis, D. Firth, A generic algorithm for reducing bias in parametric estimation. *Electron. J. Stat.* **4**, 1097 (2010). doi:10.1214/10-EJS579

29. M. C. Hansen *et al*., Global percent tree cover at a spatial resolution of 500 meters: First results of the MODros. Inf. Serv. vegetation continuous fields algorithm. *Earth Interact.* **7**, 1 (2003). doi:10.1175/1087-3562(2003)007<0001:GPTCAA>2.0.CO;2